

Self-consistent electronic structure of Mo(001) and W(001) surfaces

S. B. Legoas,* A. A. Araujo, and B. Laks

Instituto de Física Gleb Wataghin, Universidade Estadual de Campinas, CP 6165, 13083-970, Campinas, SP, Brazil

A. B. Klautau and S. Frota-Pessôa

Instituto de Física, Universidade de São Paulo, CP 66318, 05315-970, São Paulo, SP, Brazil

(Received 9 August 1999)

We report results for the surface band structures of molybdenum and tungsten (001) surfaces by employing the surface version of the first-principles, self-consistent real-space linear muffin-tin orbital method in the atomic sphere approximation. The surface state dispersions as well as the spectral density of states were obtained employing the transfer matrix scheme. The resulting surface band structures are compared with recent experimental measurements at temperatures above the transition temperature, as well as theoretical self-consistent calculations.

I. INTRODUCTION

In recent years, research in metallic systems with two-dimensional symmetry such as thin films, surfaces and multilayers has been focused primarily on the transition metals, because of their interesting properties and their technological importance. These systems have been studied experimentally by several techniques.¹ Compared to the semiconductor surfaces, transition-metal surfaces are much more difficult to treat theoretically because of the coexistence of the localized d electrons and the delocalized sp electrons. Up to now, several methods²⁻⁸ have been developed to calculate surface electronic structure self-consistently for transition metal systems. Most of these first-principles methods require perfect two-dimensional symmetry, but some of the approaches allow for the inclusion of substitutional impurities or clusters of impurities.^{5,9-11}

In this paper we use the first-principles, self-consistent real-space (RS) linear muffin-tin orbital (LMTO) formalism in the atomic sphere approximation (ASA) to determine the electronic structure of perfect (001) surfaces of Mo and W. The RS-LMTO-ASA scheme¹² is based on the well-known LMTO formalism¹³ and uses the recursion method¹⁴ to solve the eigenvalue problem directly in real space. The scheme has recently been extended to treat metallic surfaces,^{7,10} with results which agree well with those obtained by other first-principles methods.

On the other hand, the transfer-matrix approach^{15,16} is a powerful method to calculate the spectral density of states for any given \vec{k} vector in the appropriate two-dimensional Brillouin zone, at any of the slabs of atomic planes forming the solid with a surface. Our interest in this method is due to the fact that the information provided by the spectral density of states is more complete than that contained in the local density of states, since we can look at a given momentum transfer parallel to the surface. The spectral density of states is a more relevant quantity than the local density of states for the analysis of, for instance, angle-resolved photoemission experiments (ARPES).^{17,18}

From the self-consistent calculation using the RS-LMTO-ASA scheme, we obtain the Hamiltonian of the metallic sys-

tem expressed in real space. It is then transformed to reciprocal space using the translational symmetry of the atomic planes parallel to the metallic surface. The \vec{k}_{\parallel} reciprocal-space Hamiltonian is then used with the transfer matrix method to obtain the spectral density of states and the surface states dispersion of the transition metal surface considered.

The Mo and W(001) surfaces have been treated in a number of theoretical¹⁸⁻²² and experimental works,^{23,24} because of their important properties and technological applications.²⁵ When the Mo(001) and W(001) surfaces are cooled, they undergo a phase transition (reconstruction) at about room temperature from the (1×1) structure to a $(\sqrt{2} \times \sqrt{2})R45^\circ$ or $c(2 \times 2)$, structure on W(001) (Debe and King,²³) and an incommensurate $c(2.2 \times 2.2)$ (Felter *et al.*²³), or a commensurate $c(7\sqrt{2} \times \sqrt{2})$ structure (Hilder *et al.*²⁴) in the case of Mo(001). These phase transitions are of great interest because they are genuinely two-dimensional effects, and occurs on surfaces suitable for detailed low-energy electron diffraction (LEED) and photoemission measurements. It is also of interest to understand the problem of the phase transition of the Mo(001) and W(001) surfaces because their structures above the transition temperatures form similar lattice structure and they have isoelectronic properties.

Recently, calculations and measurements have been carried out to account for the driving mechanism of the surface reconstruction in Mo(001) and W(001).²⁶ One proposed mechanism involves the formation of surface charge-density waves.²⁷ This model requires the existence of a surface state in the $\bar{\Gamma}\bar{M}$ direction of the surface Brillouin zone, which crosses the Fermi level at the midpoint of the $\bar{\Sigma}$ symmetry line. Holmes and Gustafsson,²⁸ using ARPES to study the W(001) surface, found a surface state to disperse up towards the Fermi level, crossing it at $\approx 0.43\bar{\Gamma}\bar{M}$. This result led to the search for the continuation of this surface state above the Fermi level using inverse photoemission spectroscopy,^{29,30} but in none of these studies was that state observed. More recent ARPES measurements by Smith *et al.*³¹ found a surface state/resonance to disperse towards the Fermi level at

$0.34 \pm 0.12 \bar{\Gamma}\bar{M}$, but they were unable to conclude whether or not it crossed the Fermi level. In recent angle-resolved ultraviolet inverse photoemission spectroscopy measurements, Collins *et al.*³² reported to have observed an unoccupied intrinsic surface state/resonance in the $\bar{\Gamma}\bar{M}$ direction of the W(001) two-dimensional Brillouin zone. The state was found just above the Fermi level, approaching halfway along $\bar{\Sigma}$ symmetry line, and dispersing toward ≈ 2 eV above the Fermi level at \bar{M} point.

In the present paper we introduce a flexible method that permits us to perform self-consistent calculations of metallic surfaces, in the framework of density-functional theory within the local density approximation (surface RS-LMTO-ASA) together with the transfer matrix method. This scheme has an advantage over other schemes because it does not require any symmetry in space, and we can use it to consider more exotic metallic surface systems such as reconstructed surfaces, where, due to the spatial extension of the distortions, supercell methods are hardly applicable. In the present work, therefore, we utilize our recently adapted surface scheme to calculate the surface band structure of Mo(100) and W(001) surfaces, as an application of our flexible real-space self-consistent method.

This paper is organized as follows: in the next section we describe the theoretical approach used in our calculations, the surface RS-LMTO-ASA scheme and the transfer-matrix method. The results and discussions are presented in Sec. III, followed in Sec. IV by our conclusions.

II. METHOD OF CALCULATION

The method we introduce here is carried out in three steps. In the first, we perform first-principles, self-consistent electronic structure calculations for the perfect bulk metallic systems using the well known RS-LMTO-ASA scheme.¹² In this way we obtain the Fermi energy (E_F) and the potential parameters of the bulk system. In the second step, the surface RS-LMTO-ASA approach⁷ is used to calculate self-consistently the electronic structure of a semi-infinite metallic system simulated by a cluster of a few thousands atoms, arranged in a number of atomic planes parallel to the (001) crystallographic plane. Here, one empty spheres plane above the metallic surface is included. It was sufficient to consider the first four atomic planes (included the empty spheres plane) in the self-consistent calculation of the potential, whereas bulk parameters (obtained in the first step) were used in the remaining planes. At the end of the self-consistent process, we obtain the electronic structure of the metallic surface as well as the other two sub-surface atomic planes.

In the third step, the self-consistent real space Hamiltonian of the metallic system, obtained in the second step, is used in the transfer matrix method to obtain the spectral density of states and the surface state dispersions. So, in the next subsections we give a brief outline of the two approaches used here.

A. The surface RS-LMTO-ASA scheme

The RS-LMTO-ASA is a linear method¹² that uses muffin tin orbitals to construct the basis and consider the space filled

with Wigner-Seitz (WS) spheres. The solutions are accurate near a given energy E_ν , usually taken at the center of gravity of the occupied part of s , p , and d bands being considered. It is based in the orthogonal representation of the LMTO-ASA formalism¹³ and therefore the Hamiltonian is written in the following form:

$$\begin{aligned} \mathcal{H} &= E_\nu + \bar{h}(1 + \bar{o}\bar{h})^{-1} \\ &= E_\nu + \bar{h} - \bar{h}\bar{o}\bar{h} + \bar{h}\bar{o}\bar{h}\bar{o}\bar{h} - \dots, \end{aligned} \quad (1)$$

where \bar{h} is a Hermitian matrix expressed in terms of the tight-binding parameters, i.e.:

$$\bar{h} = \bar{C} - E_\nu + \bar{\Delta}^{1/2} \bar{S} \bar{\Delta}^{1/2}, \quad (2)$$

where \bar{C} , $\bar{\Delta}$, and \bar{o} are potential parameters in the tight-binding LMTO-ASA representation and \bar{S} is the structure constant in the same representation.

Here we use the second-order approximation, which neglects terms of order of $(E - E_\nu)^3$ and higher in the Hamiltonian. In this context the orthogonal Hamiltonian \mathcal{H} can be written as

$$\mathcal{H} = E_\nu + \bar{h} - \bar{h}\bar{o}\bar{h}, \quad (3)$$

and the eigenvalue problem has the form

$$(\mathcal{H} - E)u = 0, \quad (4)$$

$$\Psi_E = \sum_{RL} [\varphi_{l\nu}(r_R) + (E - E_\nu)\dot{\varphi}_{l\nu}(r_R)] Y_L(\hat{r}_R) u_{RL}(E).$$

In the nonrelativistic case, the functions $\varphi_{l\nu}(r)$ [and corresponding energy derivatives $\dot{\varphi}_{l\nu}(r)$] are solutions of the Schrödinger-like equation at each inequivalent WS sphere, at energy E_ν , while in the scalar relativistic approximation they are solutions of a simplified Dirac equation, in which the spin-orbit coupling is not included. The eigenvalue problem of Eq. (4) is solved in real space, using the recursion method.¹⁴

The RS-LMTO-ASA scheme described above can be applied to crystalline systems,¹² impurities in metallic hosts,³³ and to other systems such as surfaces.^{7,10} The basic procedure is the same in all cases, but the electrostatic potential V_{es} and the Fermi level must be determined according to the system being studied. In the case of surfaces, the Fermi level of the semi-infinite metallic system is fixed to the respective bulk value. Moreover, to make it possible to determine in a self-consistent manner the distribution of charge in the vicinity of the surface, we include one or two overlayers of empty spheres covering the surface. Having fixed the Fermi level, we can integrate the local density of states (LDOS) and determine the charge transfer at each WS sphere, including those associated with empty spheres.

In the present case, where we have only translational symmetry along the planes parallel to surface, the electrostatic potential V_{es} at each sphere is obtained by considering the multipole contribution of the potential, plus the charge in the

sphere itself. The multipole contribution is calculated using a two-dimensional (2D) Ewald technique in analogy with the usual 3D case.³

The RS-LMTO-ASA codes for crystalline metallic systems^{11,12} are available upon request. In the case of surfaces and impurities, due to the complexity of these systems that lack periodicity, some training should be arranged previous to the transfer of the codes.

B. The transfer-matrix method

Knowing that the original translational symmetry due to the lattice is retained within each layer of atoms parallel to the surface and is broken only along the perpendicular axis which might have no symmetry at all, we can investigate the surface state dispersion by analyzing the spectral density of surface states.

We take the usual picture of a cleaved surface as a collection of layers of atoms parallel to the direction of the surface. In the present case we consider a two-atom basis, such that each layer contains two atomic planes. Our Hamiltonian is written in a simple tight-binding form in the Wannier representation $|n\vec{R}_n\nu\rangle$, where n is the index of the layer, being $n=0$ for the surface layer, and \vec{R}_n is a two-dimensional vector on the layer that defines the position of a cell, while the position of the atom within the primitive cell is indicated by \vec{T}_ν . Since two-dimensional periodicity is retained within each layer, we can define Bloch states corresponding to the Wannier states above by using two-dimensional reciprocal vectors \vec{k} :

$$|n\vec{k}\nu\rangle = \frac{1}{\sqrt{N_2}} \sum_{\vec{R}_n} e^{-i\vec{k}\cdot(\vec{R}_n+\vec{T}_\nu)} |n\vec{R}_n\nu\rangle, \quad (5)$$

where N_2 is the total number of lattice points in the layer. So we write our Hamiltonian as

$$H = \sum_{n=0} \sum_{\vec{k}} \sum_{\nu\mu} \{ |n\vec{k}\nu\rangle H_{\nu\mu}(n,\vec{k}) \langle n\vec{k}\mu| + \sum_{n' \neq n} |n'\vec{k}\nu\rangle H_{\nu\mu}(n',n,\vec{k}) \langle n\vec{k}\mu| \}, \quad (6)$$

where

$$H_{\nu\mu}(n,\vec{k}) = \sum_{\vec{R}_n} e^{i\vec{k}\cdot(\vec{R}_n+\vec{T}_\nu-\vec{T}_\mu)} \mathcal{H}_{\nu\mu}(n\vec{R}_n, n\vec{0}), \quad (7)$$

$$H_{\nu\mu}(n',n,\vec{k}) = \sum_{\vec{R}_{n'}} e^{i\vec{k}\cdot(\vec{R}_{n'}+\vec{T}_\nu-\vec{T}_\mu)} \mathcal{H}_{\nu\mu}(n'\vec{R}_{n'}, n\vec{0}).$$

In the above expressions, the interaction Hamiltonians between the neighbor atoms are determined self-consistently as explained in the previous section. Defining the one-electron resolvent by

$$\mathcal{G}(z) = (z - H)^{-1},$$

where H is the total Hamiltonian and z is a complex variable, the partial spectral density of states for the subband μ corresponding to the n th layer is obtained as

$$\rho_\mu(n,\vec{k},E) \equiv -\frac{1}{\pi} \text{Im} \langle n\vec{k}\mu | \mathcal{G}(E+i0^+) | n\vec{k}\mu \rangle. \quad (8)$$

The spectral density of states (SDOS) is obtained by summing over the different types of orbitals. The Green-function matrix elements which appear on the SDOS are found from the solution of Dyson's equation

$$z\mathcal{G}(z) = 1 + H\mathcal{G}(z). \quad (9)$$

As the relaxation effects include only the first two layers (four atomic planes), the Hamiltonian matrices defined by Eqs. (7) satisfy the properties

$$H_{\nu\mu}(n,\vec{k}) = H_{\nu\mu}(b,\vec{k}), \quad (10a)$$

$$H_{\nu\mu}(n',n,\vec{k}) = H_{\nu\mu}(n'-n,b,\vec{k}), \quad n, n' \geq 3, \quad (10b)$$

where the matrices $H(b,\vec{k})$ and $H(n,b,\vec{k})$ are constructed from the bulk calculations.

From the Dyson's equation (9) we obtain an infinite set of coupled equations that can be solved by using the transfer-matrix method. In the case of the surface layer the infinite set of equations are

$$\begin{aligned} [z - H(0,\vec{k})] \mathcal{G}_{00} &= 1 + H(0,1,\vec{k}) \mathcal{G}_{10}, \\ [z - H(1,\vec{k})] \mathcal{G}_{10} &= H(1,0,\vec{k}) \mathcal{G}_{00} + H(1,2,\vec{k}) \mathcal{G}_{20}, \\ &\vdots \\ [z - H(b,\vec{k})] \mathcal{G}_{n0} &= H(1,b,\vec{k}) \mathcal{G}_{n-1,0} \\ &\quad + H(-1,b,\vec{k}) \mathcal{G}_{n+1,0}, \quad n \geq 3. \end{aligned} \quad (11)$$

The solution of this set of equations can be found by introducing a transfer matrix $\mathbb{T}(z,\vec{k})$, independent of n , defined by

$$\mathcal{G}_{n+1,m}(z,\vec{k}) = \mathbb{T}(z,\vec{k}) \mathcal{G}_{nm}(z,\vec{k}), \quad n \geq m. \quad (12)$$

Inserting this definition into the motion equations (11) we get the following equation for the transfer matrix:

$$H(-1,b,\vec{k}) \mathbb{T}^2 + [H(b,\vec{k}) - z] \mathbb{T} + H(1,b,\vec{k}) = 0.$$

Once the transfer matrix is obtained we can compute the SDOS for all layers.

III. RESULTS AND DISCUSSION

We have used the surface RS-LMTO-ASA scheme⁷ to perform first-principles, density-functional electronic structure calculations for perfect Mo(001) and W(001) surfaces. The von Barth and Hedin parametrization form³⁴ to the exchange and correlation term of the energy potential was used. For the case of the Mo(001) surface, a nonrelativistic calculation was performed, while for the W(001) surface a scalar relativistic calculation was carried out. A basis of s , p , and d orbitals at each site was chosen to describe the

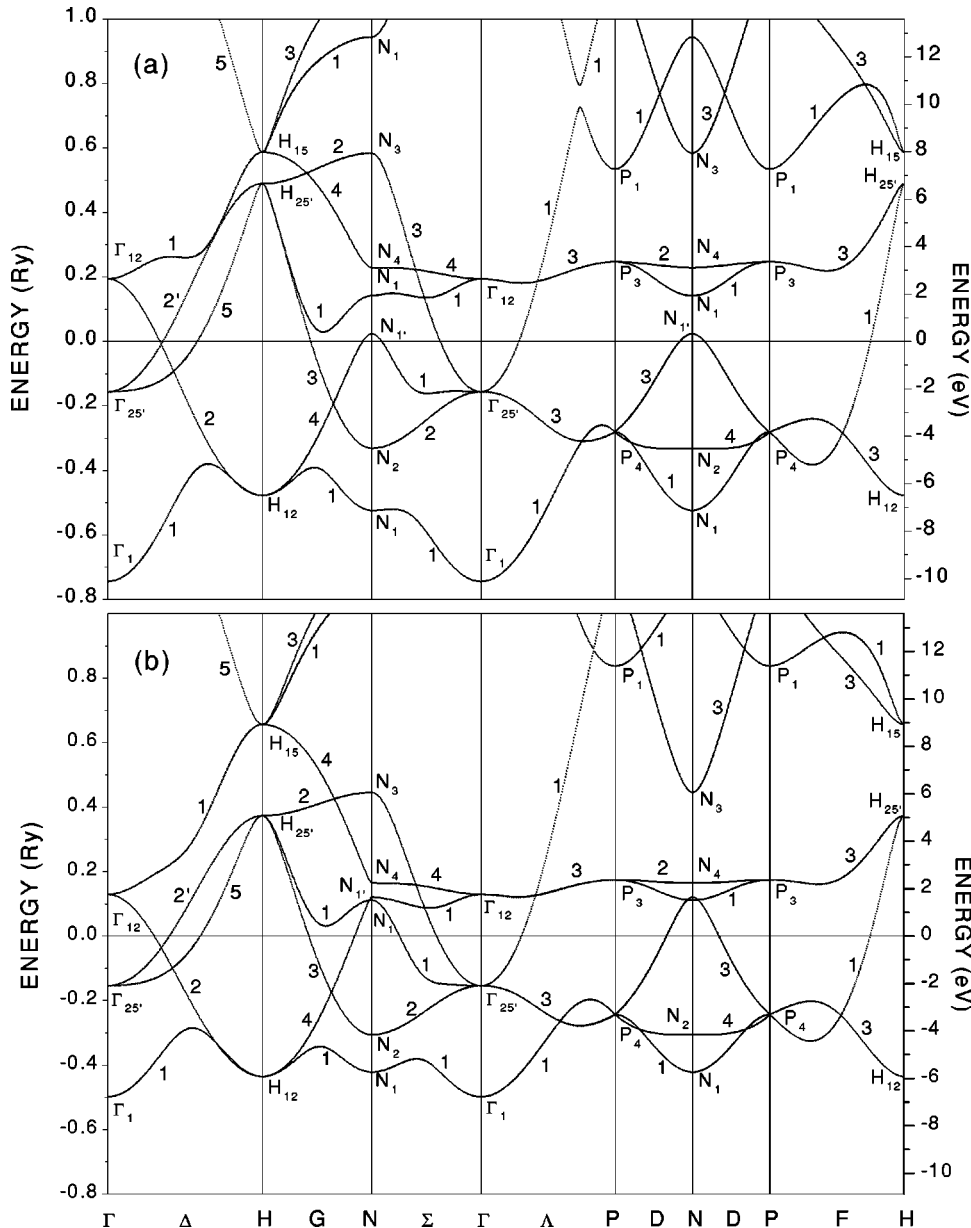


FIG. 1. Band structure of (a) W and (b) Mo as calculated using the RS-LMTO-ASA method. For tungsten a scalar relativistic calculation was performed, while a non-relativistic treatment was considered for Mo. The energy scale is relative to Fermi level of each metal.

valence band, but in the case of W, fully occupied $4f$ orbitals were included in the core. The use of f electrons in the basis set significantly increases the computational effort while leading to an f occupation of around 0.15 electrons¹³ and therefore only small changes in the occupied part of the band. The inclusion of $l=3$ states in the basis may be of importance for a correct description of the higher states in the empty band. Self-consistency was assumed when the difference between the input and output occupations was less than 1×10^{-3} electrons. A cluster of ≈ 2200 atoms, arranged in 13 atomic planes parallel to the (001) surface, was used in the surface calculations. As was outlined in Sec. II, in the self-consistent process it was sufficient to consider four atomic planes: one empty spheres overlayer, a metallic surface, and two subsurface metallic planes to calculate their potential parameters, while for the remaining planes bulk parameters were taken. Lattice parameters of 5.9478 and 5.9814 a.u. for Mo and W, respectively, were used. A contraction of the topmost surface layer spacing was not considered, and the surface layer had the (1×1) bulk symmetry.

A. Mo bulk and W bulk

In Sec. II, a self-consistent bulk calculation was pointed out to be necessary prior to the self-consistent surface electronic-structure calculations. In the case of Mo and W we have used the standard RS-LMTO-ASA scheme,¹² including the second order $\bar{h}\bar{o}\bar{h}$ term in the Hamiltonian matrix, and the same exchange-correlation term as in the surface calculation was taken. The cluster size was of ≈ 4300 sites, and 21 coefficients in the recursion step were used. Nonrelativistic and scalar relativistic calculations were performed for Mo and W, respectively. The same criterium of convergence and lattice parameters was used as for the surface calculations.

In Fig. 1 and Table I, the band structures and energy band eigenvalues of Mo and W are shown. The overall agreement between our results and those obtained by other methods is rather good.

In Table II we compare our results for the \vec{k} vectors of the Fermi surfaces of Mo and W with other results from the literature. For Mo we can note that the \vec{k} vectors of the el-

TABLE I. Comparison of energy band eigenvalues with respect to Fermi level (in Ry) of molybdenum and tungsten, as obtained by other authors and by us. Nonrelativistic (NR) and semirelativistic (SR) calculations for Mo and W were carried out.

	Mo		W		W	
	NR ^a	NR ^b	NR ^c	SR ^d	SR ^e	SR ^c
Γ_1	0.488	0.54	0.50	0.73	0.688	0.75
$\Gamma_{25'}$	0.080	0.10	0.15	0.11	0.086	0.16
Γ_{12}	0.108	0.104	0.13	0.14	0.166	0.20
H_{12}	0.403	0.42	0.435	0.45	0.421	0.48
$H_{25'}$	0.285	0.29	0.37	0.36	0.371	0.49
H_{15}	0.699	0.67	0.66	0.59	0.620	0.59
N_1	0.372	0.40	0.42	0.48	0.449	0.52
N_2	0.228	0.25	0.31	0.28	0.259	0.33
$N_{1'}$	0.122	0.11	0.11	0.03	0.084	0.02
N_1				0.10	0.159	0.14
N_4	0.161	0.16	0.16	0.23	0.226	0.23
N_3	0.337	0.35	0.44	0.43	0.440	0.58
P_4	0.179	0.20	0.24	0.24	0.207	0.28
P_3	0.169	0.17	0.17	0.22	0.237	0.25
P_1	0.795	0.72	0.83	0.46	0.486	0.53
$N_{1'} - \Gamma_1$	0.61	0.65	0.61	0.76	0.772	0.77
$H_{25'} - H_{12}$	0.688	0.71	0.80	0.81	0.79	0.97

^aReference 51.

^bReference 52.

^cPresent work.

^dReference 53.

^eReference 54.

lipsoids (E), hole octahedron (O), and electron jack (J) are in reasonable agreement with the experiments. In the case of W it is easy to appreciate the difference between the results of scalar and full relativistic calculations, owing to the effect of the spin-orbit interaction in the electron jack and the hole octahedron.

TABLE II. Experimental and theoretical values of the \vec{k} vectors of Fermi surface of molybdenum and tungsten (in \AA^{-1}).

	Mo			W			
	Theor. ^a	Theor. ^b	Expt. ^c	Theor. ^a	Theor. ^d	Theor. ^e	Expt. ^f
$J_{\Gamma H}$	1.20	1.15	1.13	1.15	1.16	1.08	1.09
$J_{\Gamma N}$	0.58	0.49	0.58	0.52	0.51	0.40	0.46
$J_{\Gamma P}$	0.52	0.44	0.47	0.48	0.47	0.36	0.41
$E_{N\Gamma}$	0.36	0.27	0.35	0.13			0.143
E_{NP}	0.34	0.37	0.40	0.16			0.195
E_{NH}	0.22	0.19	0.20	0.11			0.121
$O_{H\Gamma}$	0.80	0.84	0.86	0.83	0.81	0.77	0.75
O_{HN}	0.60	0.63	0.60	0.62	0.60	0.59	0.60
O_{HP}	0.44	0.53	0.50	0.43	0.50	0.49	0.50

^aPresent work. Nonrelativistic (Mo) and semirelativistic (W) calculations.

^bReference 55.

^cReference 56.

^dReference 57.

^eReference 58.

^fReference 59.

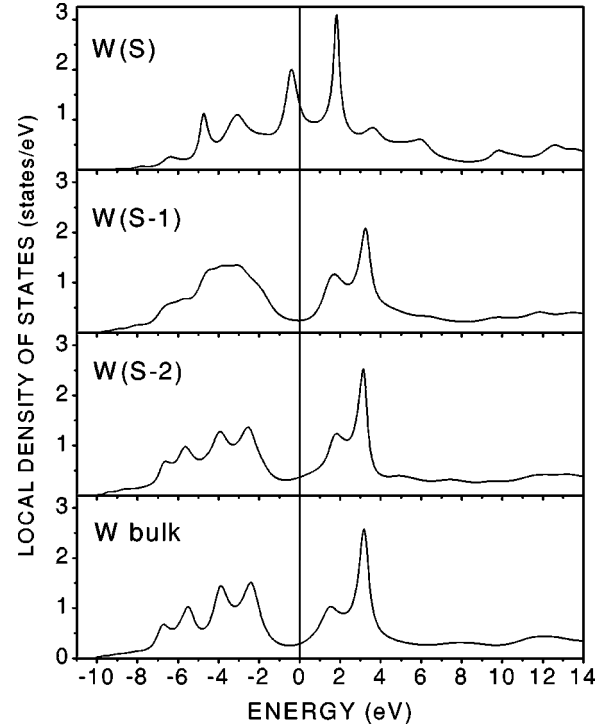


FIG. 2. Total local density of states ($s+p+d$) for the W(001) surface, W(S), nearest-neighbor atomic plane W(S-1), next-nearest-neighbor atomic plane W(S-2), and W bulk. Energy axis is relative to Fermi level.

B. W(001) surface

One of the most important results of the self-consistent calculation is the local density of states (LDOS). Figure 2 shows the LDOS of the W(001) surface, the two subsurface layers, and the W bulk. At the surface, we readily identify two prominent high-lying features, one occupied at -0.39 eV and one unoccupied at 1.8 eV. The occupied high-lying peak corresponds to the well known peak observed in field-emission energy distribution (FEED) measurements (Swanson and Crouser,^{35(a)} Plummer and Gadzuk²³), as well as in the energy distribution of photoelectrons emitted from W(001) surfaces.^{36,37} The unoccupied high-lying peak may correspond to the feature found by Drube *et al.*²⁹ in their inverse photoemission measurements (IPES). As Fig. 2 shows, the peak at -0.39 eV is located in the deep valley below the Fermi level of the W bulk. The subsurface layers have also this deep valley at the same position. This surface state is composed mainly of $yz=zx$ and x^2-y^2 orbitals. The 1.8 -eV peak presents mainly $3z^2-r^2$ orbital character and results from the lifting of the degeneracy of the e_g states of the bulk because of the lack of periodicity of the potential along the z direction.

The low-lying peak at -4.7 eV corresponds to the feature observed by Feuerbacher and Fitton²⁴ using the energy distribution spectra of photoelectrons, as well as by Lapeyre *et al.*³⁸ and Weng *et al.*³⁹ using ARPES and angle-resolved synchrotron photoemission, respectively. This feature is composed mainly of s , x^2-y^2 , and $3z^2-r^2$ orbitals. The peak at -3.1 eV corresponds to the surface state/resonance (SR when the state does not have a clear surface state character) observed by Campuzano *et al.*⁴⁰ using ARPES measurements.

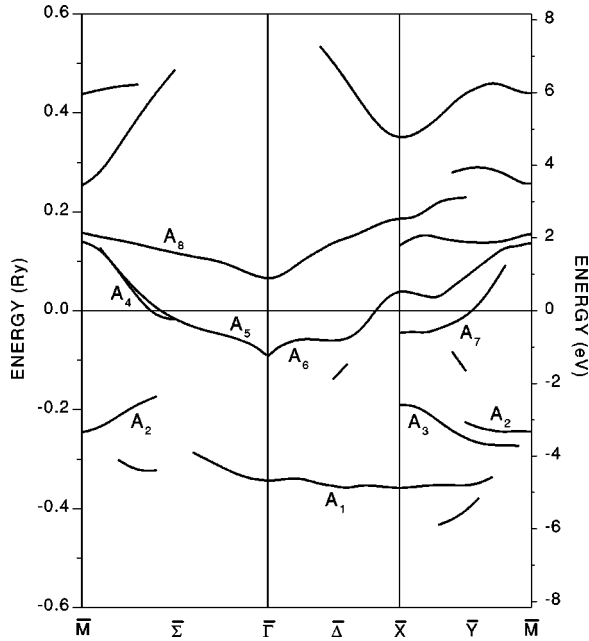


FIG. 3. Surface state dispersion curves for W(001) surface as obtained considering a scalar relativistic treatment. Main symmetry lines of the surface Brillouin zone have been considered. The energy axis is relative to Fermi level.

All these results shown by the LDOS curve (Fig. 2), may be observed in more detail in the surface state dispersion curves (Fig. 3). The band labeled A_1 contributes to the low-lying peak at -4.7 eV observed in the LDOS curve. This band has predominantly $3z^2 - r^2$ character in the $\bar{\Gamma}\bar{M}$ and $\bar{\Gamma}\bar{X}$ directions. In the region near the \bar{X} point it changes to s character, and so it follows along the \bar{Y} symmetry line. As was indicated above, this band was observed by Campuzano *et al.*,⁴⁰ along the symmetry line $\bar{\Sigma}$ starting in the $\bar{\Gamma}$ point. Recently, Elliot *et al.*,⁴¹ using their high-resolution angle-resolved photoemission measurements of the high-temperature phase of W(001), have obtained the whole band labeled A_1 (S_1 in their notation) along the $\bar{\Sigma}$, $\bar{\Delta}$, and \bar{Y} lines, in good agreement with the present results. Moreover, the A_2 band, which contributes to the features at -3.1 eV, was obtained along the $\bar{\Sigma}$ and \bar{Y} lines, as shown in Fig. 3. These A_1 and A_2 bands were also found by Mattheis and Hamann⁴² and Posternak *et al.*,⁴³ utilizing the self-consistent scalar relativistic linearized augmented plane-wave (LAPW) method on an unrelaxed seven-layer W(001) slab. In the Fermi level region, we obtain the A_6 band along the $\bar{\Delta}$ as found by Elliot *et al.*⁴¹ (S_5 in their notation), including the crossing of E_F at $k_{\parallel} = 0.83 \text{ \AA}^{-1}$. Posternak *et al.*⁴³ also obtained some SR states along the $\bar{\Delta}$ line just below E_F ; however, the dispersion as well as the point where they cross E_F are different from those of Elliot *et al.*⁴¹ and from our results. At the $\bar{\Sigma}$ line we obtain a band labeled A_5 that starts near $\bar{\Gamma}$ point and disperses towards the Fermi level, crossing it at $0.57 \bar{\Gamma}\bar{M}$, reaching the \bar{M} point at 1.9 eV above the Fermi energy. This band exhibits a split (A_4) in the E_F region, crossing it at $0.64 \bar{\Gamma}\bar{M}$. Similar results were obtained

by Mattheis and Hamann⁴² and by Posternak *et al.*,⁴³ as well as by Ohnishi *et al.*⁴⁴ Experimentally, Campuzano *et al.*⁴⁰ and Holmes and Gustafsson²⁸ found similar bands at the $\bar{\Sigma}$ symmetry line, one of them with the same property of crossing the Fermi level at approximately the midpoint of the $\bar{\Gamma}\bar{M}$ line. However, recently ARPES measurements⁴⁵ showed no crossing bands along the $\bar{\Sigma}$ line, in agreement with Elliot *et al.*⁴¹

On the other hand, utilizing angle-resolved IPES, it has recently been possible to map the unoccupied energy levels of the W(001) surface. It is interesting to compare, as is often done in the literature, the theoretical results with photoemission experiments, but one must be aware of the limitations of the LDA approximation. A discussion of this point can be found in Ref. 46 which studies surface resonances on Ta(001). They conclude that for materials near the beginning of the transition metal series the position of the states will be given approximately correctly by band calculations. Mo and W, like Ta, are early transition metals and comparisons between LDA calculations and experiments are often found in the literature. But even so some differences between theory and experiment regarding the position of the states are to be expected. Drube *et al.*²⁹ obtained inverse photoemission spectra along $\bar{\Sigma}$ symmetry line, showing an SR band that begins at the $\bar{\Gamma}$ point with ≈ 0.5 eV and disperses away from $\bar{\Gamma}$ up to 1.4 eV at $k_{\parallel} = 0.8 \bar{\Gamma}\bar{M}$ [Fig. 1(b), Ref. 29]. Our surface state dispersion curves (Fig. 3) show an unoccupied SR band (designed as A_8) that closely corresponds to that of Drube *et al.* This A_8 band comes near the \bar{M} point with a small dispersion and has predominantly $3z^2 - r^2$ character in all its extension. Our results show that A_8 band continues along $\bar{\Delta}$ line showing reasonable dispersion, reaching the \bar{X} point with 2.5 eV. More recently, Collins *et al.*³² obtained an IPES spectra of the W(001) surface at room temperature, showing an SR band in the $\bar{\Gamma}\bar{M}$ direction above the Fermi level. These results differ from those of Drube *et al.* mainly in the energy position of the states, smaller in the case of Collins *et al.* Comparing with our results, we can conclude that the unoccupied surface states obtained by Collins *et al.* may be considered to be the A_8 band. An orbital character determination of that surface state might give an experimental confirmation of our assertion. Finally, Lamouri and Krainsky⁴⁷ presented IPES results of unoccupied surface states of W(001) near the Fermi level in the $\bar{\Gamma}\bar{M}$ direction. Their measurements differ strongly from those of Drube *et al.*, but are similar to those of Collins *et al.* In Fig. 3 we can see that along $\bar{\Delta}$ and \bar{Y} symmetry lines appear other SR bands above E_F . These unoccupied SR have not been experimentally observed to date.

In this paper we use the scalar relativistic approximation, where the effect of spin-orbit coupling is neglected. There are indications that spin-orbit effects may slightly modify the dispersion curves of the W(001) surface close to E_F .⁴² Even so, most calculations in the literature, including relatively recent ones,²⁶ neglect the spin orbit coupling when treating the valence band. We should note that there are no intrinsic limitations regarding the inclusion of spin-orbit effects in the

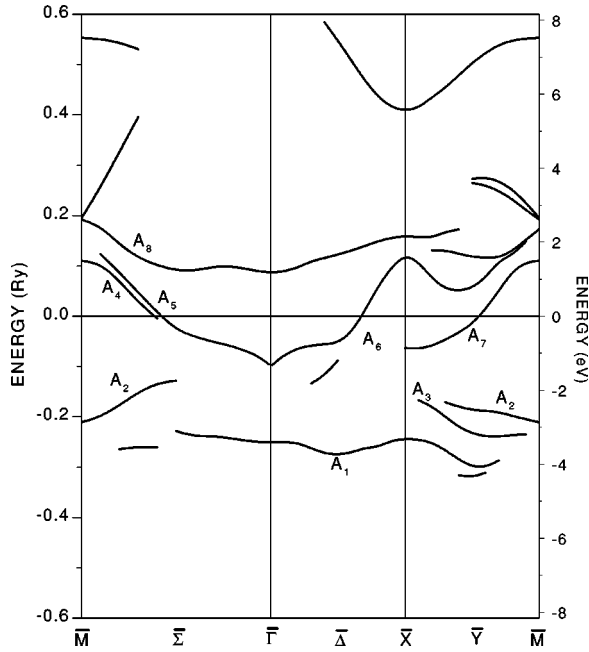


FIG. 4. Surface state dispersion curves for the Mo(001) surface. In this case a nonrelativistic treatment was considered, the same as used for the Mo bulk. The symmetry lines showed correspond to the main ones of the surface Brillouin zone. The energy axis is relative to Fermi level.

RS-LMTO-ASA approach. In fact, the inclusion of spin-orbit coupling along the lines suggested by Eriksson *et al.*⁴⁸ can be conveniently incorporated into the real space codes.

C. Mo(001) surface

In comparison to all the studies of the W(001) surface, in the case of the molybdenum (001) surface considerably fewer theoretical and experimental investigations have been reported. Our results for the Mo(001) surface are shown in Fig. 4. We can see that the SR band structure of Mo is very similar to that of tungsten. We have identified some SR bands in the same way as Kerker *et al.*²⁰ [in their self-consistent pseudopotential calculation for an unrelaxed Mo(001) surface]. However, differences appear with respect to the extent of the bands along the symmetry lines. For instance, the A_1 band extends along all the $\bar{\Delta}$ line up to approximately the midpoint of the $\bar{\Sigma}$ line. This is not the case of Kerker's results. Comparing with the self-consistent semi-relativistic FP-LAPW calculation of Hong and Chung,²¹ we note that they did not obtain the A_1 band along the $\bar{\Sigma}$ line except for some states near the $\bar{\Gamma}$ point. In the ARPES measurements of Smith and Kevan,⁴⁹ it is easy to observe the extension of the A_1 band in the direction $\bar{\Gamma}\bar{M}$ as found in this work. At this point we have to indicate that along the $\bar{\Delta}$ line our results show a single band that begins in the $\bar{\Gamma}$ point and runs all along the $\bar{\Delta}$ line up to the \bar{X} point, while the results of Smith and Kevan show two bands, one that begins in the $\bar{\Gamma}$ point with a high dispersion towards E_F , and another one that begins at the \bar{X} point with less dispersion in the opposite direction than the first band.

In the energy region around 2 eV below the Fermi level, we find a band labeled as A_2 that begins in the \bar{M} point and disperses towards E_F along the \bar{Y} and $\bar{\Sigma}$ lines. Kerker *et al.* obtain the A_2 band (F in their notation) along the \bar{Y} line without a beginning at the \bar{M} point, and they have not observed this band in $\bar{M}\bar{\Gamma}$ direction. Hong and Chung found this band beginning at the \bar{M} point and dispersing towards E_F along the \bar{Y} and $\bar{\Sigma}$ lines, but with less extension that we have calculated. Shin *et al.*,⁵⁰ using ARPES, also obtained this band in the direction $\bar{M}\bar{\Gamma}$.

We now look into the details of the dispersion relations in the region near and below E_F . Initially, we will compare our relations along \bar{Y} line with the calculations of Kerker *et al.* and of Hong and Chung. We obtain the band labeled A_7 in the same way as Kerker *et al.* (E_3 in their notation). Hong and Chung also obtained this band. In the $\bar{\Gamma}\bar{X}$ direction our results show a single band labeled A_6 that begins near the $\bar{\Gamma}$ point and disperses towards E_F , crossing it at $0.71 \bar{\Gamma}\bar{X}$. This band has zx and $x^2 - y^2$ orbital character. A similar band was obtained in the case of W(001), crossing the Fermi level at $0.84 \bar{\Gamma}\bar{X}$. The results of Kerker *et al.* are very different from this work; they obtained a strong double SR band labeled E_1 and E_2 along the $\bar{\Delta}$ line, but without its crossing the Fermi level. The ARPES measurements of Smith and Kevan show an SR band in the $\bar{\Gamma}\bar{X}$ direction, very different from our results. Along the $\bar{\Gamma}\bar{M}$ direction, our double SR band, labeled A_4 and A_5 , is very similar to that of Kerker *et al.*, but in our case this band disperses up to \bar{M} point at 1.4 eV above E_F . Hong and Chung also obtained this band, noting that it crosses the Fermi level at $0.61 \bar{\Gamma}\bar{M}$ in good agreement with our results ($0.60 \bar{\Gamma}\bar{M}$). The SR band along the $\bar{\Sigma}$ line of Smith and Kevan behaves in a similar way to our A_4, A_5 band, and crosses E_F at $0.65 \bar{\Gamma}\bar{M}$. Our results show that the A_4 band has mainly $3z^2 - r^2$ and xy orbital character, while the A_5 band has predominantly $x^2 - y^2$ and $xz = yz$ character.

As we have explained the study of the spectral density of states gives information about the surface state dispersion curves. In Fig. 5 we show the results for the spectral density of states of Mo at four special points along the symmetry line $\bar{\Sigma}$, for three different (001) planes: surface plane (full line), the plane immediately below it (thin dashed line), and a plane in the bulk of the material (thick dotted line). At the $\bar{\Gamma}$ point, Fig. 5(a), there is a noticeable peak at 3.4 eV below the Fermi level. This A_1 peak, which has predominantly $3z^2 - r^2$ character, has been detected and interpreted as a surface state. Above the Fermi level we see a prominent peak labeled A_8 , that belongs to the A_8 band in Fig. 4. Just below E_F we observe some states that mix with bulk states and do not develop a peak at the $\bar{\Gamma}$ point. As we move along the $\bar{\Sigma}$ symmetry line, Fig. 5(b), in addition to the peak present at $\bar{\Gamma}$, we found a new peak (A_5) situated about 0.4 eV below the Fermi level. Both t_{2g} and e_g orbitals contribute to its spectral

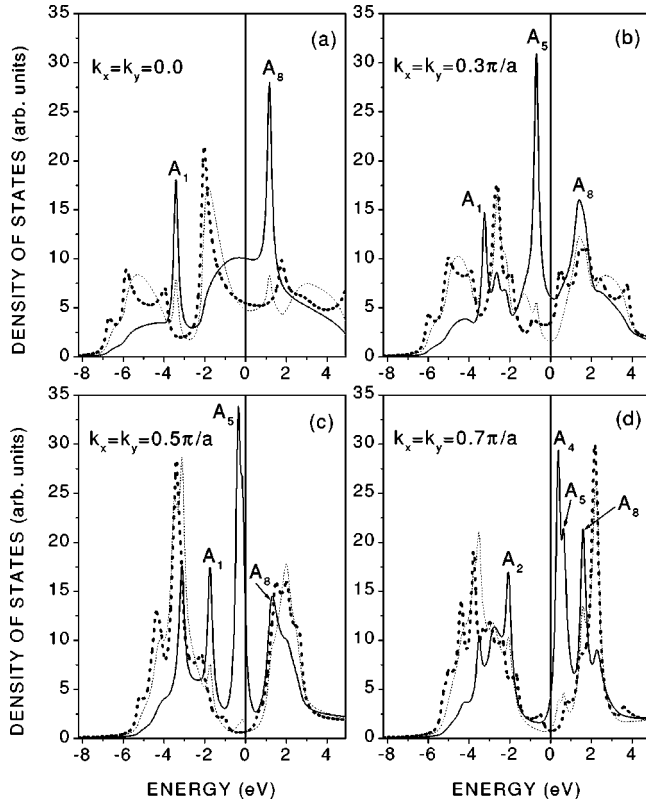


FIG. 5. Spectral density of states for Mo on the surface plane (full line), second plane (thin dashed line), and bulk plane (thick dotted line) along the $\bar{\Sigma}$ symmetry line: (a) $\bar{\Gamma}$ point; (b) $k_x = k_y = 0.3\pi/a$; (c) $k_x = k_y = 0.5\pi/a$; (d) $k_x = k_y = 0.7\pi/a$. The structures labeled as A_1, \dots , correspond to the SR states shown in Fig. 4. The Fermi level is taken as reference.

density. At the midpoint of the $\bar{\Sigma}$ line, Fig. 5(c), this peak has moved to the Fermi level and a shoulder appears on its high-energy side. This structure is well defined in Fig. 5(d). The two peaks A_4 and A_5 correspond to the splitting of the resonance state and are located in a hybridization gap in its associated bulk band structure. Such a splitting is not observed along the $\bar{\Gamma}\bar{X}$ direction because the hybridization gap is not open here. This can be seen in Fig. 6, where we show the amplitude of the surface states versus \vec{k} values for the two directions in the 2D Brillouin zone. As one can see, most of the charge density associated with these resonances is confined to a small region in the vicinity of $|\vec{k}| = 0.35 \pi/a$.

At this time there are no reported measurements of unoccupied states for the Mo(001) surface. However, our nonrelativistic calculations show an SR band structure above the Fermi level, similar to the case of W(001) surface.

IV. CONCLUSIONS

We have introduced an alternative way of determining self-consistently, from first-principles, the electronic structure and spectral densities around metallic surfaces. The method does not require structural symmetry along the direction perpendicular to the surface and can be applied to investigate the effect of surface reconstruction on surface states

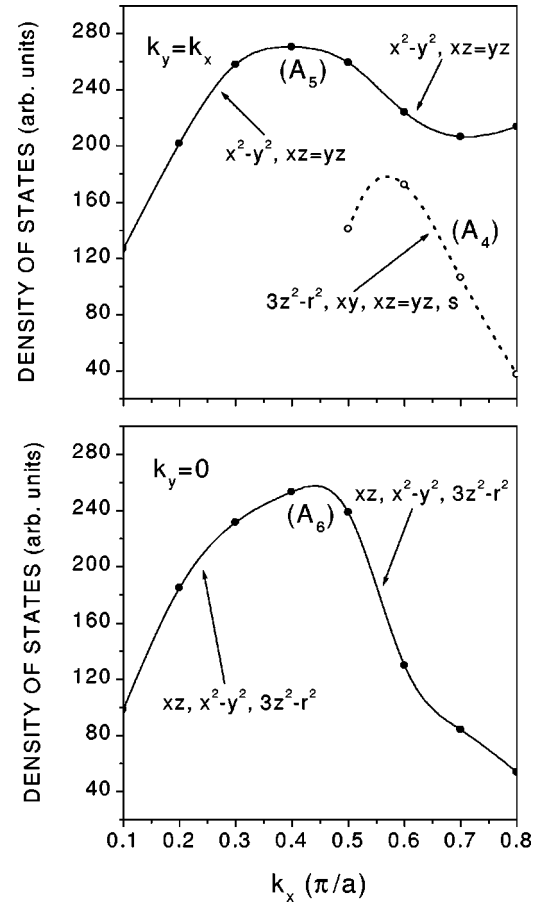


FIG. 6. Amplitude variation of the high-lying occupied resonances along the symmetry lines (a) $\bar{\Sigma}$; (b) $\bar{\Delta}$ in the 2D Brillouin zone for Mo(001) surface. The arrows indicate the orbital character, decreasing from left to right.

and resonances. The proposed scheme combines first-principles real-space electronic structure calculations (RS-LMTO-ASA) with the transfer-matrix method and has been applied here to study Mo(001) and W(001) surfaces. We note that, in order to obtain a better description of empty states, second-order terms $\bar{h}\bar{o}\bar{h}$ were included in the RS-LMTO-ASA Hamiltonian.

We verify that our results for the electronic structure of bulk Mo and W follow closely those obtained by other methods. The surface description is also in reasonable agreement with experimental observations and other calculations. For M(001) and W(001) surfaces our results show an SR state at energies close to E_F , along the $\bar{\Sigma}$ symmetry line, crossing the Fermi level nearly at the midpoint of this line. This state is seen to split into the A_4 and A_5 bands. Similar results have also been obtained in other theoretical works.^{20,21,42-44} It has been suggested that this behavior may be responsible for the observed surface reconstructions of Mo(001) and W(001) surfaces as explained by surface charge-density waves theory. For the W(001) surface we find a low-lying SR state (labeled A_1), along the $\bar{\Sigma}$, $\bar{\Delta}$, and \bar{Y} symmetry lines, in good agreement with experiment (Elliot *et al.*⁴¹). Our results also show an SR state (A_6) in the Fermi level region, along the $\bar{\Delta}$ line, again in good agreement with the results of Elliot *et al.*

Finally, in the $\bar{\Gamma}\bar{M}$ direction, above the Fermi level, we find an SR state (A_8) that corresponds to the unoccupied SR state found experimentally with IPES.^{29,32}

We calculate the spectral density of states for the symmetry directions in the 2D \vec{k} space for both Mo(001) and W(001) surfaces. The spectral density of states gives a precise characterization of the surface states regarding their symmetry and their localization both in real space and in the 2D Brillouin zone. Within this approach the character of the resonant states is readily identified. In the case of Mo(001) surface the calculation was able to show a splitting of the

surface state labeled A_5 along the $\bar{\Gamma}\bar{M}$ direction, as well as the change in the involved orbital character.

ACKNOWLEDGMENTS

This work was supported by the Fundação de Amparo à Pesquisa do Estado de São Paulo (FAPESP), and the CNPq (Brazil). The authors are grateful to W.D. Brewer of the Freie Universitaet Berlin for his comments regarding the manuscript.

- *Author to whom correspondence should be addressed. FAX: +55-19-7885376. Electronic address: slegoas@ifi.unicamp.br
- ¹S. Weng, E.W. Plummer, and T. Gustafsson, Phys. Rev. B **18**, 1718 (1978); W.A. Macedo and W. Keine, Phys. Rev. Lett. **61**, 475 (1988); G. Schatz, X.L. Ding, R. Fink, G. Krausch, B. Luckscheiter, R. Platzler, J. Voigt, U. Wöhrmann, and R. Weische, Hyperfine Interact. **60**, 975 (1990); S.S.P. Parkin, N. More, and K.P. Roche, Phys. Rev. Lett. **64**, 2304 (1990).
 - ²C.L. Fu and A.J. Freeman, Phys. Rev. B **35**, 925 (1987).
 - ³H.L. Skriver and N.M. Rosengaard, Phys. Rev. B **43**, 9538 (1991).
 - ⁴P. Lang, L. Nordström, R. Zeller, and P.H. Dederichs, Phys. Rev. Lett. **71**, 1927 (1993).
 - ⁵I. Turek, J. Kudrnovský, V. Drchal, and P. Weinberger, Phys. Rev. B **49**, 3352 (1994).
 - ⁶T. Kraft, P.M. Marcus, and M. Scheffler, Phys. Rev. B **49**, 11 511 (1994).
 - ⁷P.R. Peduto and S. Frota-Pessôa, Braz. J. Phys. **27**, 574 (1997).
 - ⁸P. Lang, V.S. Stepanyuk, K. Wildberger, R. Zeller, and P.H. Dederichs, Solid State Commun. **92**, 755 (1994).
 - ⁹V.S. Stepanyuk, W. Hergert, K. Wildberger, R. Zeller, and P.H. Dederichs, Phys. Rev. B **53**, 2121 (1996).
 - ¹⁰A.B. Klautau, P.R. Peduto, and S. Frota-Pessôa, J. Magn. Magn. Mater. **186**, 223 (1998).
 - ¹¹A.B. Klautau, S.B. Legoas, R.B. Muniz, and S. Frota-Pessôa, Phys. Rev. B **60**, 3421 (1999).
 - ¹²P.R. Peduto, S. Frota-Pessôa, and M.S. Methfessel, Phys. Rev. B **44**, 13 283 (1991).
 - ¹³O.K. Andersen, Phys. Rev. B **12**, 3060 (1975); O.K. Andersen and O. Jepsen, Phys. Rev. Lett. **53**, 2571 (1984); O.K. Andersen, O. Jepsen, and D. Glötzel, in *Highlights of Condensed Matter Theory*, edited by F. Bassani, F. Funi, and M.P. Tosi (North-Holland, Amsterdam, 1985).
 - ¹⁴R. Haydock, in *Solid State Physics*, edited by H. Ehrenreich, F. Seitz, and D. Turnbull (Academic Press, New York, 1980), Vol. 35, p. 215.
 - ¹⁵L.M. Falicov and F. Ynduram, J. Phys. C **8**, 1563 (1975).
 - ¹⁶C.E.T. Gonçalves da Silva and B. Laks, J. Phys. C **10**, 851 (1977).
 - ¹⁷B. Feuerbacher and R.F. Willis, Phys. Rev. Lett. **36**, 1339 (1976).
 - ¹⁸B. Laks and C.E.T. Gonçalves da Silva, Solid State Commun. **25**, 401 (1978).
 - ¹⁹R.V. Kasowski, Solid State Commun. **17**, 179 (1975); M.C. Desjonquères and F. Cyrot-Lackmann, *ibid.* **26**, 271 (1978).
 - ²⁰N.V. Smith and L.F. Mattheis, Phys. Rev. Lett. **37**, 1494 (1976); G.P. Kerker, K.M. Ho, and M.L. Cohen, *ibid.* **40**, 1593 (1978).
 - ²¹S.C. Hong and V.W. Chung, Phys. Rev. B **48**, 4755 (1993); L.D. Roelofs and S.M. Focles, *ibid.* **48**, 11 287 (1993).
 - ²²I.G. Batirev, H. Hergert, P. Rennert, V.S. Stepanyuk, T. Oguchi, A.A. Katsnelson, J.A. Leiro, and K.H. Lee, Surf. Sci. **417**, 151 (1998).
 - ²³E.W. Plummer and J.W. Gadzuk, Phys. Rev. Lett. **25**, 1493 (1970); W.F. Egelhoff, Jr., J.W. Linnet, and D.L. Perry, *ibid.* **36**, 98 (1976); S.L. Weng, *ibid.* **38**, 434 (1977); M.K. Debe and D.A. King, *ibid.* **39**, 708 (1977); T.E. Felter, R.A. Barker, and P.J. Estrup, *ibid.* **38**, 1138 (1977).
 - ²⁴B. Feuerbacher and B. Fitton, Solid State Commun. **15**, 295 (1974); R.F. Willis, B. Feuerbacher, and B. Fitton, *ibid.* **18**, 1315 (1976); M.L. Hildner, R.S. Daley, T.E. Felter, and P.J. Estrup, J. Vac. Sci. Technol. A **9**, 1604 (1991).
 - ²⁵Z.Y. Li, R.N. Lamb, W. Allison, and R.F. Willis, Surf. Sci. **211/212**, 931 (1989); G. Wu, B. Bartlett, and W.T. Tysoe, *ibid.* **383**, 57 (1997); G. Wu and W.T. Tysoe, *ibid.* **391**, 134 (1997); K. Ota, M. Tanaka, and S. Usami, *ibid.* **402-404**, 813 (1998); R. de Coss, Surf. Rev. Lett. **3**, 1505 (1996).
 - ²⁶R. Yu, H. Krakauer, and D. Singh, Phys. Rev. B **45**, 8671 (1992).
 - ²⁷E. Tosatti and P.W. Anderson, Solid State Commun. **14**, 773 (1974); E. Tosatti, *ibid.* **25**, 637 (1978).
 - ²⁸M.I. Holmes and T. Gustafsson, Phys. Rev. Lett. **47**, 443 (1981).
 - ²⁹W. Drube, D. Straub, F.J. Himpsel, P. Soukiassian, C.L. Fu, and A.J. Freeman, Phys. Rev. B **34**, 8989 (1986).
 - ³⁰I.L. Krainsky, J. Vac. Sci. Technol. A **5**, 735 (1987).
 - ³¹K.E. Smith, G.S. Elliot, and S.D. Kevan, Phys. Rev. B **42**, 5385 (1990).
 - ³²I.R. Collins, H.D. Laine, and P.T. Andrews, J. Phys.: Condens. Matter **4**, 2891 (1992).
 - ³³S. Frota-Pessôa, Phys. Rev. B **46**, 14 570 (1992); H.M. Petrilli and S. Frota-Pessôa, *ibid.* **48**, 7148 (1993).
 - ³⁴V. von Barth and L. Hedin, J. Phys. **12**, 141 (1982).
 - ³⁵L.W. Swanson and L.C. Crouser, (a) Phys. Rev. Lett. **16**, 389 (1966); (b) **19**, 1179 (1967).
 - ³⁶B.J. Waclawski and E.W. Plummer, Phys. Rev. Lett. **25**, 1493 (1970).
 - ³⁷B. Feuerbacher and B. Fitton, Phys. Rev. Lett. **29**, 786 (1972).
 - ³⁸G.J. Lapeyre, R.J. Smith, and J. Anderson, J. Vac. Sci. Technol. **14**, 384 (1977).
 - ³⁹S.L. Weng, T. Gustafsson, and E.W. Plummer, Phys. Rev. Lett. **39**, 822 (1977).
 - ⁴⁰J.C. Campuzano, D.A. King, C. Somerton, and J.E. Inglesfield, Phys. Rev. Lett. **45**, 1649 (1980).
 - ⁴¹G.S. Elliott, K.E. Smith, and S.D. Kevan, Phys. Rev. B **44**, 10 826 (1991).
 - ⁴²L.F. Mattheis and D.R. Hamann, Phys. Rev. B **29**, 5372 (1984).

- ⁴³M. Posternak, H. Krakauer, A.J. Freeman, and D.D. Koelling, Phys. Rev. B **21**, 5601 (1980).
- ⁴⁴S. Ohnishi, A.J. Freeman, and E. Wimmer, Phys. Rev. B **29**, 5267 (1984).
- ⁴⁵K.S. Shin, H.W. Kin, and J.W. Chung, Surf. Sci. **385**, L978 (1997).
- ⁴⁶X. Pan, E.W. Plummer, and M. Weinert, Phys. Rev. B **42**, 5025 (1990).
- ⁴⁷A. Lamouri and I.L. Krainsky, Surf. Sci. **303**, 341 (1994).
- ⁴⁸O. Eriksson, B. Johansson, R.C. Albers, A.M. Boring, and M.S.S. Brooks, Phys. Rev. B **42**, 2702 (1990).
- ⁴⁹K.E. Smith and S.D. Kevan, Phys. Rev. B **45**, 13 642 (1992).
- ⁵⁰K.S. Shin, C.Y. Kim, J.W. Chung, S.C. Hong, S.K. Lee, C.Y. Park, T. Kinoshita, M. Watanabe, A. Kakizaki, and T. Ishii, Phys. Rev. B **47**, 13 594 (1993).
- ⁵¹I. Petroff and C.R. Viswanathan, Phys. Rev. B **4**, 799 (1971).
- ⁵²D.A. Papaconstantopoulos, *Handbook of the Band Structure of Elemental Solids* (Plenum Press, New York, 1986).
- ⁵³L.F. Mattheis and D.R. Hamann, Phys. Rev. B **29**, 5372 (1984).
- ⁵⁴D.M. Bylander and L. Kleinman, Phys. Rev. B **27**, 3152 (1983).
- ⁵⁵T.L. Loucks, Phys. Rev. **139**, A1181 (1965) (nonrelativistic calculation).
- ⁵⁶G. Leaver and A. Myers, Philos. Mag. **19**, 465 (1969).
- ⁵⁷L.F. Mattheis and R.E. Watson, Phys. Rev. Lett. **13**, 526 (1964) (semirelativistic calculation).
- ⁵⁸T.L. Louks, Phys. Rev. **143**, 506 (1966) (full relativistic APW calculation).
- ⁵⁹V.V. Boiko and V.A. Gasparov, Zh. Éksp. Teor. Fiz. **61**, 2363 (1972) [Sov. Phys. JETP **34**, 1266 (1972)].